



ELSEVIER

Contents lists available at ScienceDirect

Data in brief

journal homepage: www.elsevier.com/locate/dib

Data Article

Stochastic simulations data for figure 1 and the phase diagram construction for defining monotonic and non-monotonic regimes of the velocity as a function of k_{off}



Divya Singh, Srabanti Chaudhury*

Department of Chemistry, Indian Institute of Science Education and Research, Dr. Homi Bhabha Road, Pune 411008, Maharashtra, India

ARTICLE INFO

Article history:

Received 29 April 2019

Received in revised form 4 June 2019

Accepted 25 June 2019

Available online 3 July 2019

Keywords:

Stochastic simulations

Phase diagram

ABSTRACT

We have compared our theoretical expressions of the normalized reaction velocities with that of simulation data points generated when the substrate fluctuations are present and absent, for the reaction schemes represented in Figure 1 Singh and Chaudhury, 2019 in the general monotonic as well as the conditional non-monotonic limit. We have also constructed the phase diagrams for the schemes given in Figure 1 Singh and Chaudhury, 2019 separating different regimes of the monotonic and the non-monotonic behaviors observed in the reaction rate.

© 2019 Published by Elsevier Inc. This is an open access article under the CC BY-NC-ND license (<http://creativecommons.org/licenses/by-nc-nd/4.0/>).

DOI of original article: <https://doi.org/10.1016/j.chemphys.2019.04.012>.

* Corresponding author.

E-mail address: srabanti@iiserpune.ac.in (S. Chaudhury).

<https://doi.org/10.1016/j.dib.2019.104211>

2352-3409/© 2019 Published by Elsevier Inc. This is an open access article under the CC BY-NC-ND license (<http://creativecommons.org/licenses/by-nc-nd/4.0/>).

Specifications table

Subject	Chemistry
Specific subject area	Theory of Single Molecule Enzyme Kinetics and Stochastic Simulations
Type of data	Figures and Equations
How data were acquired	Theory and Simulations
Data format	Analyzed
Parameters for data collection	The reaction velocity from the stochastic simulations as a function of the unbinding rate constant in the presence and absence of substrate fluctuations and the phase diagram for separating different velocity regimes (a theoretical approach)
Description of data collection	Stochastic simulations using Gillespie Algorithm were performed to obtain the reaction velocity. We followed a mathematical procedure for the phase diagram construction.
Data source location	Institution: Indian Institute of Science Education and Research (IISER), Pune City/Town/Region: Pune Country: India
Data accessibility	With the article
Related research article	Author's name: D. Singh, S. Chaudhury Title: Theoretical study of the conditional non-monotonic off rate dependence of catalytic reaction rates in single enzymes in the presence of conformational fluctuations Journal: Chemical Physics DOI: https://doi.org/10.1016/j.chemphys.2019.04.012

Value of the data

- The theoretical studies are performed under the excess substrate assumption [1] where the reaction rates are calculated at short times. We perform the stochastic simulations [2] under the constant substrate approximation and also incorporate the effect of substrate fluctuations and compare with the theoretical results for the reaction schemes described in Fig. 1 [1]. This data helps in understanding the agreement/deviation between the formulated theory and the datasets obtained from the numerical simulations under different physical scenarios.
- The theoretical investigations and simulation datasets provide a platform for dynamical interpretations of enzymatic networks taken under consideration. Our data can assist and validate studies based on single molecule measurements.
- Using these backgrounds one can extend similar systems to some more complicated reaction schemes subjected to the conformational fluctuations.
- We have constructed the phase diagram [3] for the schematic represented in Fig. 1 [1] separating different regimes of the reaction velocity.

1. Data

We have compared the normalized reaction velocities from theory and simulations for the reaction schemes represented in Fig. 1 [1] at a fixed value of substrate concentration (shown in Fig. 1 of this article) as a function of k_{off} and $k_{off}^{(1)}$, respectively. We have also performed a comparative study between the normalized rates from theory and simulations for those schemes [1] at a given [S] under the non-monotonic limit (represented in Fig. 2 of this article) as a function of k_{off} and $k_{off}^{(1)}$, respectively.

2. Experimental design, materials, and methods

2.1. Comparison of the theoretical expressions for the normalized velocity with the stochastic simulations for a general parameter set

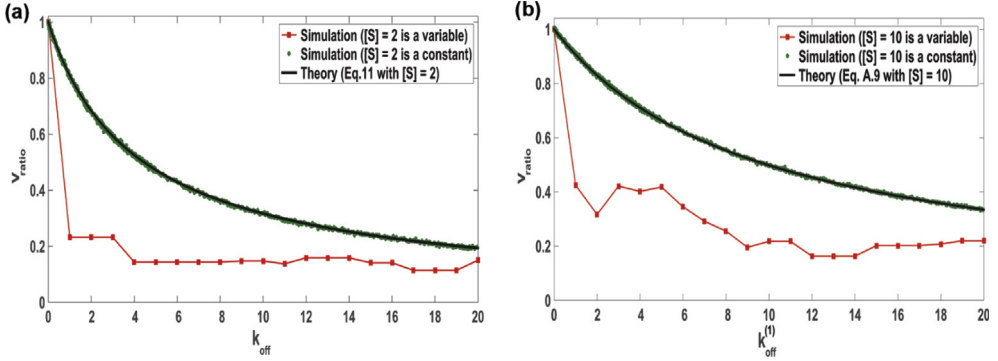


Fig. 1. (a) Comparison of the normalized reaction velocity from theory and simulations for the reaction scheme represented in (a) Fig. 1(a) [1] at $[S] = 2$. The reaction rate constants are $k_{on} = 1$, $\alpha = 1$, $\beta = 2$, and $k_{cat} = 5$. (b) Fig. 1(b) [1] at $[S] = 10$, as a function of k_{off} and $k_{off}^{(1)}$, respectively. The reaction rate constants are $k_{on} = 1$, $\alpha = 1$, $\beta_1 = 2$, $\beta_2 = 4$ and $k_{cat} = 5$. The red solid lines represent the stochastic simulations carried out taking $[S]$ as a variable (filled red squares are the generated data points), the filled green circles represent the simulation points at constant $[S]$ and the black solid lines represent Eq. 11 and Eq. A.9 [1] in (a) and (b), respectively.

2.2. Comparison of the theoretical expressions for the normalized velocity with the stochastic simulations in the non-monotonic limit

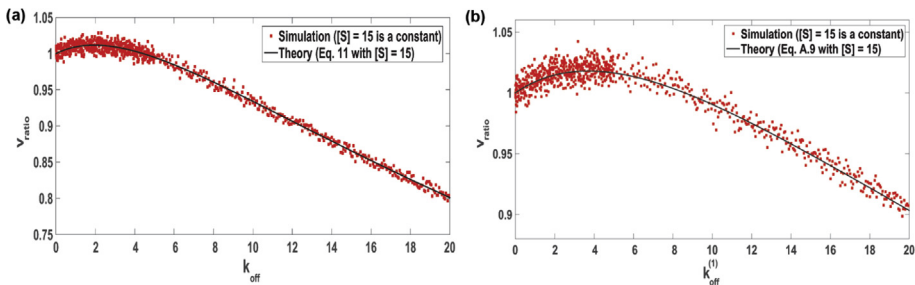


Fig. 2. Comparison of the normalized reaction velocity in the non-monotonic limit for the reaction scheme represented in (a) Fig. 1(a) [1] at $[S] = 15$ with $k_{cat} > \frac{16\alpha\beta^2}{(\alpha-\beta)^2}$, $\alpha > \beta$. The set of reaction rate constants are $k_{on} = 1$, $\alpha = 3$, $\beta = 1$ and $k_{cat} = 20$. (b) Fig. 1 (b) [1] at $[S] = 15$ with $\left(k_{cat} > \frac{16\alpha\beta_1\beta_2}{(\alpha-\beta_2)^2}, \alpha > \beta_2\right)$, as a function of k_{off} and $k_{off}^{(1)}$, respectively. The set of reaction rate constants in the plot are $k_{on} = 1$, $\alpha = 4$, $\beta_1 = 2$, $\beta_2 = 1$ and $k_{cat} = 25$. The filled red squares represent the stochastic simulation data points obtained when $[S]$ is taken as a constant and the black solid lines represent Eq. 11 and A.9 [1] in (a) and (b), respectively.

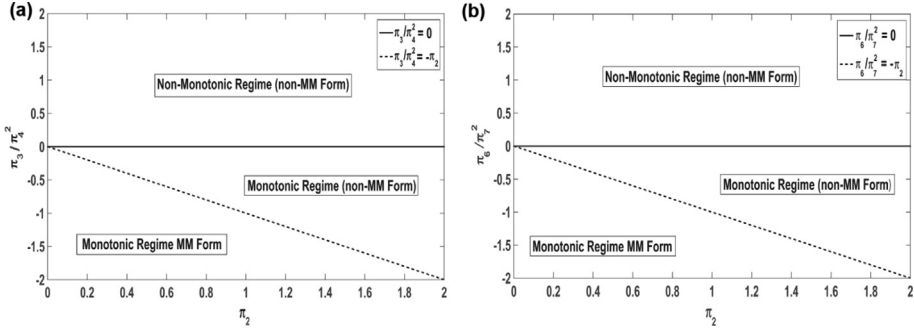


Fig. 3. Phase diagram separating different regions of the normalized reaction velocity for the reaction scheme represented in (a) Fig. 1(a) [1] where the solid black line and the dashed black line represent $\frac{\pi_3}{(\pi_4)^2} = 0$ and $\frac{\pi_3}{(\pi_4)^2} = -\pi_2$, respectively (b) in Fig. 1(b) [1] where the solid black line and the dashed black line represent $\frac{\pi_6}{(\pi_7)^2} = 0$ and $\frac{\pi_6}{(\pi_7)^2} = -\pi_2$, respectively.

2.3. Mathematical procedure followed for the phase diagram construction

Rearranging eq 10 [1] in terms of the unbinding rate constant k_{off} we get

$$v_{1P} = \left(\pi_1 + \pi_2 k_{off} + \frac{\pi_3}{k_{off} + \pi_4} \right)^{-1} \quad (1)$$

where,

$$\pi_1 = 2 \left(\frac{1}{k_{cat}} + \frac{1}{k_{on}[S]} \right), \quad \pi_2 = \frac{2}{k_{cat}k_{on}[S]}, \quad \pi_3 = 1 - \frac{\beta}{\alpha} - \frac{2\beta}{k_{on}[S]} \text{ and } \pi_4 = \beta \left(2 + \frac{k_{on}[S]}{\alpha} \right).$$

Differentiating v_{1P} (eq (1)) with respect to k_{off} and putting the limit $k_{off} \rightarrow 0$, we get

$$\left(\frac{dv_{1P}}{dk_{off}} \right)_{k_{off} \rightarrow 0} = \frac{\frac{\pi_3}{(\pi_4)^2} - \pi_2}{\left(\pi_1 + \frac{\pi_3}{\pi_4} \right)^2} \quad (2)$$

For the general set of kinetic parameters, we find that $\left(\frac{dv_{1P}}{dk_{off}} \right)_{k_{off} \rightarrow 0} < 0$ as $\frac{\pi_3}{(\pi_4)^2} < \pi_2$. Thus, the reaction velocity is a continuously decreasing function of k_{off} as shown in Fig. 2(a).

We solve eq 13 [1] and obtain a particular range of $[S]$ in which non-monotonicity in the velocity is observed and the parameter values satisfy the limits mentioned in eq 14a and eq 14b [1]. As shown in

Fig. 2(b), the velocity derivative with respect to k_{off} $\left(\frac{\pi_3}{(\pi_4)^2} > \pi_2 \right)$ increases initially and then decreases

$\left(\frac{\pi_3}{(\pi_4)^2} < \pi_2 \right)$. To construct the phase diagram (Fig. 3(a)) that can separate different monotonic and non-monotonic regions of velocity, we plot $\frac{\pi_3}{(\pi_4)^2}$ as a function of π_2 . We define the non-monotonicity index (\emptyset) as

$$\emptyset = \frac{\frac{\pi_3}{(\pi_4)^2}}{\pi_2} \quad (3)$$

If $\varnothing > 1$, it represents the region in which the velocity will show a non-monotonic (non-MM) behavior. As discussed in the main text, this will be observed only in a certain range of the substrate concentration with some particular choice of parameter values.

$0 < \varnothing \leq -1$ represents the regime in which the velocity will show a monotonic (non-MM) behavior for any given set of kinetic parameters. When $\varnothing < -1$ it represents the region in which the velocity attains the MM form and decreases monotonically.

For Fig. 1(b), rearranging eq 12 [1] in terms of the unbinding rate constant $k_{off}^{(1)}$ we get

$$v_{2P} = \left(\pi_5 + \pi_2 k_{off}^{(1)} + \frac{\pi_6}{k_{off}^{(1)} + \pi_7} \right)^{-1} \quad (4)$$

where,

$$\pi_2 = \frac{2}{k_{cat}k_{on}[S]}, \quad \pi_5 = \frac{\beta_1 + \beta_2}{\beta_2 k_{cat}} + \frac{2}{k_{on}[S]}, \quad \pi_6 = \beta_1 \left(-\frac{1}{\alpha} + \frac{1}{\beta_2} - \frac{2}{k_{on}[S]} \right) \text{ and } \pi_7 = \beta_1 \left(2 + \frac{k_{on}[S]}{\alpha} \right)$$

Differentiating eq (4) with respect to $k_{off}^{(1)}$ and putting the limit $k_{off}^{(1)} \rightarrow 0$, we get

$$\left(\frac{dv_{2P}}{dk_{off}^{(1)}} \right)_{k_{off}^{(1)} \rightarrow 0} = \frac{\frac{\pi_6}{(\pi_7)^2} - \pi_2}{\left(\pi_5 + \frac{\pi_6}{\pi_7} \right)^2} \quad (5)$$

The non-monotonic velocity will only be observed if $\frac{\pi_6}{(\pi_7)^2} > \pi_2$. Otherwise, the reaction velocity will show a monotonic behavior when studied as a function of $k_{off}^{(1)}$.

We construct the phase diagram as shown in Fig. 3(b) separating different regions of velocity and plot $\frac{\pi_6}{(\pi_7)^2}$ as a function of π_2 . For the scheme represented in Fig. 1(b), the non-monotonicity index is defined as

$$\varnothing' = \frac{\frac{\pi_6}{(\pi_7)^2}}{\pi_2} \quad (6)$$

As described earlier, $\varnothing' > 1$, $0 < \varnothing' \leq -1$ and $\varnothing' < -1$ represent regime with non-monotonic (non-MM), monotonic (non-MM) and monotonic MM behavior, respectively. We have constructed a phase diagram which divides different regions of the reaction rate (depicted in Fig. 3 of this article).

Acknowledgments

The authors acknowledge support from IISER Pune. DS acknowledges IISER Pune and CSIR for the scholarship. SC acknowledges DST-SERB grant GAP/DST/CHE-15-184 for funding.

Conflict of interest

The authors declare that they have no known competing financial interests or personal relationships that could have appeared to influence the work reported in this paper.

References

- [1] D. Singh, S. Chaudhury, Theoretical study of the conditional non-monotonic off rate dependence of catalytic reaction rates in single enzymes in the presence of conformational fluctuations, *Chem. Phys.* 523 (2019) 150–159.
- [2] D.T. Gillespie, Exact stochastic simulation of coupled chemical reactions, *J. Phys. Chem.* 81 (25) (1977) 2340–2361.
- [3] D.E. Piephoff, J. Wu, J. Cao, Conformational nonequilibrium enzyme kinetics: generalized michaelis–menten equation, *J. Phys. Chem. Lett.* 8 (15) (2017) 3619–3623.